Metabolomics

MAIMS: A GAIMS alternative for the deconvolution of UDP-N-acetyl-D-glucosamine 13C mass isotopologue profiles
--Manuscript Draft--

Manuscript Number:	
Full Title:	MAIMS: A GAIMS alternative for the deconvolution of UDP-N-acetyl-D-glucosamine 13C mass isotopologue profiles
Article Type:	Short Communication
Keywords:	metabolic tracer analysis; stable isotope resolved metabolomics; UDP-GlcNAc; isotopologue deconvolution; endothelial cells; combinatorial optimization
Corresponding Author:	Dries Verdegem VIB - KULeuven Leuven, BELGIUM
Corresponding Author Secondary Information:	
Corresponding Author's Institution:	VIB - KULeuven
Corresponding Author's Secondary Institution:	
First Author:	Dries Verdegem
First Author Secondary Information:	
Order of Authors:	Dries Verdegem
	Hunter NB Moseley
	Wesley Vermaelen
	Abel Acosta Sanchez
	Bart Ghesquière
Order of Authors Secondary Information:	
Funding Information:	

15/03/17 9:14 AM

1

MAIMS: A GAIMS ALTERNATIVE FOR THE DECONVOLUTION OF UDP-N-ACETYL-D-GLUCOSAMINE ^{13}C MASS ISOTOPOLOGUE PROFILES

Dries Verdegem[1,2], Hunter NB Moseley[3], Wesley Vermaelen[1,2], Abel Acosta Sanchez[1,2] & Bart Ghesquière[1,2]

(1) Metabolomics Expertise Center, VIB Center for Cancer Biology (CCB), VIB, Leuven, B-3000, Belgium; (2) Metabolomics Expertise Center, Department of Oncology, KU Leuven, Leuven, B-3000, Belgium; (3) Department of Molecular and Cellular Biochemistry, University of Kentucky, Lexington, Kentucky, United States of America

Corresponding author: B. Ghesquière, Ph.D.
Metabolomics Expertise Center
Center for Cancer Biology
VIB, KU Leuven, Campus Gasthuisberg O&N4
Herestraat 49 - 912,
B-3000, Leuven, Belgium
tel: 32-16-32.27.33; fax: 32-16-37.25.85

e-mail: bart.ghesquiere@kuleuven.vib.be

MAIMS: A GAIMS ALTERNATIVE FOR THE DECONVOLUTION OF UDP-N-ACETYL-D-GLUCOSAMINE ^{13}C MASS ISOTOPOLOGUE PROFILES

ABSTRACT

INTRODUCTION: Metabolic Tracer Analysis (MTA) is a collection of principles, rules and tools for the interpretation of stable isotope incorporation patterns. One example is the GAIMS algorithm for the deconvolution of the UDP-GlcNAc ^{13}C mass isotopologue profile. GAIMS has been presented as a powerful, yet currently unavailable, proof-of-concept-only technique.

OBJECTIVES: We aimed to build a tool inspired by the original GAIMS algorithm and providing identical functionality.

METHODS: We implemented MAIMS by applying Multistart metaheuristics combined with an efficient hybrid stopping rule to solve the non-convex optimization underlying the deconvolution problem. By testing our tool on several theoretical datasets, we were able to confirm its robust and reproducible performance.

RESULTS: MAIMS is capable of finding the individual contributions of specifically labeled glucose, ribose, acetyl and uracil moieties to UDP-GlcNAc upon U-^{13}C-glucose administration and thereby hinting on the activity of several metabolic pathway activities. Applied to proliferating endothelial cells (ECs), MAIMS lead to several interesting metabolic insights.

CONCLUSION: MAIMS is a powerful and extendible tool for isotopologue deconvolution tasks and is freely available on github as an open-source python (python 2.7 and 3 compliant) script for command line usage. (http://github.com/savantas/MAIMS).

KEYWORDS

Metabolic tracer analysis, stable isotope resolved metabolomics, UDP-GlcNAc, isotopologue deconvolution, endothelial cells, combinatorial optimization

INTRODUCTION

O-Linked β-N-acetylglucosamine (O-GlcNAc) signaling is being recognized as an important factor in the maintenance of metabolic homeostasis through its cell signaling, gene transcription and translation actions and epigenetic reprogramming (Bond and Hanover 2015; Ruan et al. 2013). Disregulation of the O-GlcNAcylation process has therefore also been implicated in several diseases with important metabolic components such as diabetes (Ma and Hart 2013), cancer (Singh et al. 2015), cardiovascular disease (Dassanayaka and Jones 2014), aging-related chronic diseases (Banerjee et al. 2016) and neurodegenerative disease (Wani et al. 2016). Interestingly, UDP-N-acetyl-D-glucosamine (UDP-GlcNAc), the precursor for O-GlcNAcylation, is generated by the hexosamine biosynthesis pathway (HBP), which relies on the cellular availability of several key energy metabolites as starting material (e.g. glucose, glutamine, UTP and acetyl-CoA) (Fig. 1) and has correspondingly been put forward as a nutrient sensing metabolite (Hardiville and Hart 2014). This not only explains its crucial role in the metabolic homeostasis process, but also made it emerge as a probe for cellular metabolism in stable isotopes resolved metabolomics (SIRM) (Moseley et al. 2011). Furthermore, UDP-GlcNAc is often (much) more abundant than its unbound metabolic building blocks, and its mass spectrometry (MS) measurement alone can therefore be more informative than the sum of the individual MS measurements.

The methodology in the SIRM field dealing with the qualitative interpretation of stable isotope (mostly ^{13}C) isotopologue patterns is Metabolic Tracer Analysis (MTA) (Buescher et al. 2015). GAIMS (Genetic Algorithm for Isotopologues in Metabolic Systems) was presented as a potentially powerful MTA tool for the deconvolution of the UDP-GlcNAc ^{13}C mass isotopologue profile into the individual contributions of glucose, ribose, uracil and acetyl-CoA (of which UDP-GlcNAc is composed) upon U-^{13}C-glucose administration (Moseley et al. 2011). Especially when performed in a time-resolved manner, GAIMS is capable of straightforwardly and elegantly providing the relative fluxes through different essential biochemical pathways involved in the biosynthesis of UDP-GlcNAc, such as

glycolysis, the pentose phosphate pathway (PPP), the TCA cycle and pyrimidine biosynthesis.

To solve the described deconvolution problem, which is in essence a non-convex optimization problem, GAIMS proposed a hybrid genetic and simulated annealing algorithm. However, it was presented as a proof-of-concept algorithm only and was not made available as usable software. Here, we present MAIMS (Multistart Algorithm for Isotopologues in Metabolic Systems), in which the optimal solution is sought by performing several local searches with random initialization (generally referred to as Multistart (Marti et al. 2013)). Even though conceptually more straightforward than the original GAIMS, this procedure was found to provide the correct deconvolution solutions in an equally robust manner.

MATERIALS AND METHODS

THE UDP-GLCNAC DECONVOLUTION MODEL

In the original GAIMS paper (Moseley et al. 2011) over 40 different UDP-GlcNAc moiety models were compared. A form of the Akaike information criterion (AIC) was used to deduce the best model amongst these, which nicely corresponded with the intuitive model, developed out of biological considerations. This optimal UDP-GlcNAc deconvolution model was defined by the following set of equations:

$$g6 = 1 - g0; \; r5 = 1 - r0; \; a2 = 1 - a0, \tag{1}$$

$$u0 + u1 + u2 + u3 = 1 \tag{2}$$

$$
\begin{aligned}
i0 &= a0g0r0u0 \\
i1 &= a0g0r0u1 \\
i2 &= a0g0r0u2 + a2g0r0u0 \\
i3 &= a0g0r0u3 + a2g0r0u1 \\
i4 &= a2g0r0u2 \\
i5 &= a0g0r5u0 + a2g0r0u3 \\
i6 &= a0g0r5u1 + a0g6r0u0 \\
i7 &= a0g0r5u2 + a0g6r0u1 + a2g0r5u0 \\
i8 &= a0g0r5u3 + a0g6r0u2 + a2g0r5u1 + a2g6r0u0 \\
i9 &= a0g6r0u3 + a2g0r5u2 + a2g6r0u1 \\
i10 &= a2g0r5u3 + a2g6r0u2 \\
i11 &= a0g6r5u0 + a2g6r0u3 \\
i12 &= a0g6r5u1 \\
i13 &= a0g6r5u2 + a2g6r5u0 \\
i14 &= a0g6r5u3 + a2g6r5u1 \\
i15 &= a2g6r5u2 \\
i16 &= a2g6r5u3 \\
i17 &= \text{Natural abundance contribution only}
\end{aligned}
\tag{3}
$$

where $g0$, $g6$, $r0$, $r5$, $a0$, $a2$, $u0$, $u1$, $u2$ and $u3$ are unlabeled glucose, U-^{13}C-glucose, unlabeled ribose, U-^{13}C-ribose, unlabeled acetyl, U-^{13}C-acetyl, unlabeled uracil, ^{13}C$_1$-uracil, ^{13}C$_2$-uracil and ^{13}C$_3$-uracil respectively and $i(0 \rightarrow 17)$ are the different theoretical UDP-GlcNAc isotopologue intensity terms. This deconvolution model is also the default model of the MAIMS tool. It is specified in a separate XML file as a series of components and constraints (see supplementary material), allowing for maximum flexibility when extensions beyond the specific UDP-GlcNAc case presented here, are desired.

MULTISTART METAHEURISTICS

Formally, the general combinatorial optimization problem to solve is specified by: $T = \sum \left| \left(I_{n,obs} - I_{n,calc} \right) \right|$, in which $I_{n,obs}$ is the experimentally observed isotopologue and $I_{n,calc}$ is specified by the deconvolution model (equations 1, 2 and 3). Again to assure maximum flexibility, the resulting optimization problem is generated is generated on the fly using the sympy module (Joyner et al. 2012) (supplementary material). The minimization thus involves sixteen isotopologue intensity difference terms with regard to six parameters: g0, r0, a0, u0, u1 and u2 (corresponding to the fractions of unlabeled glucose, ribose, acetyl-CoA and uracil and single and double labeled uracil in UDP-GlcNAc, respectively). This cost function may be characterized by large numbers of local minima with very small regions of attraction (number of starting points leading to that minimum), in which case it constitutes a significant challenge for the metaheuristic algorithm applied to find the global minimum. Importantly, the parameters represent fractions, meaning only values within logical fraction boundaries should be considered ($g0, r0, a0, u0, u1, u2 \in [0,1]$).

To solve the minimization problem, MAIMS applies the Multistart metaheuristic. This is an iterative procedure, in which each iteration starts with randomly chosen values for the fractional parameters within the mentioned boundaries, followed by the search for a local minimum given that initial point in the search domain. As local search method, three algorithms from the SciPy.Optimize module capable of bound constrained minimization (L-BFGS-B, TNC and SLSQP) are provided (Jones 2001 -). By default, Sequential Least SQuares Programming (SLSQP) is used because of its fast convergence. The best local minimum found during the iterative search is returned as the final solution to the deconvolution problem.

STOPPING RULES

Iterative global optimization procedures are proceeded until some predefined criterion of optimality is satisfied. Such criteria (often formally derived from mathematical/statistical considerations) are typically described by so-called stopping rules, which cue for a halt whenever the probability of not yet having reached the global minimum has become acceptably low. However, their usefulness mostly lies in the fine-tunable trade-off they offer between reliability and computational effort. Several stopping rules have been defined (Dick 2014), three of which were found to be compatible with the isotopologue deconvolution problem:

- **I/ROA (5000/20)**: This most simple rule specifies that both (a) the total number of iterations and (b) the region

of attraction (ROA; number of starting points leading to that minimum) of the best local minimum should each reach a specific predefined threshold (chosen to be 5000 and 20, respectively).

- **Boender3 (10000)**: The third Boender rule (Boender and Kan 1987) is defined as: $E(L_3) = c_3(w/(n-1)) + n$, in which n is the number of local searches performed so far and w is the current number of different local minima found. It expresses a Bayes' theorem derived loss function to minimize and consists of two terms: (a) the termination loss ($w/(n-1)$), which is proportional to the number of unobserved local minima and (b) the execution loss (n) which corresponds to the cost of performing additional iterations. Both terms are balanced by a scaling factor (c_3), which was set to 10000 during our evaluation. We chose to end the Multistart procedure when the loss function estimate ($E(L_3)$) increased for ten consecutive iterations.

- **HCS (0.4/0.4)**: Applying the high confidence stopping rule (Dick 2014) means to stop performing new iterations when:

$$\frac{|\mathcal{F}_n^1|}{n} + (2\sqrt{2} + \sqrt{3})\sqrt{\frac{ln\left(\frac{3}{\delta}\right)}{n}} < c \tag{4}$$

Here, n is again the number of local searches performed and $|\mathcal{F}_n^1|/n$ is the fraction of local minima observed exactly once. The left side of the inequality forms a proven upper bound of the missing mass (the global probability of currently unobserved local minima) with a probability of at least $1 - \delta$. Hence, the HCS rule incites of stopping as soon as the missing mass is smaller than a predefined value (c) with a probability determined by δ, with $c, \delta \in]0,1[$. For the current deconvolution problem, c and δ were both set to 0.4.

EVALUATION DATA

To evaluate the reproducibility and robustness of both the Multistart and stopping rule aspects of the MAIMS algorithm, we generated 3 x 9 = 27 artificial datasets as input for the tool. These datasets (supplementary tables 1, 3 and 5) were generated by: (1) randomly generating three different sets of feasible values for the parameters to optimize (g0, r0, a0, u0, u1, u2) ($d1$, $d2$ and $d3$), (2) based on these values, calculating the theoretical UDP-GlcNAc isotopologue profiles using equations 1, 2 and 3 ($d1.t$, $d2.t$ and $d3.t$) and (3) from each of these theoretical isotopologues, generating eight (2 x 4) other profiles by randomly drawing new values for each isotopologue signal (m0, m1, ..., m17) from a normal distribution with increasing standard deviations (0.001, 0.002, 0.01 and 0.1) around the theoretical signal

intensities ($d1.r1 \rightarrow 8$, $d2.r1 \rightarrow 8$ and $d3.r1 \rightarrow 8$). They mimic an experimental situation in which measuring errors (of different possible magnitudes) will inevitably occur. Any values outside the range [0,1] were clipped.

CELL CULTURE AND LC-MS

The cell culture and LC-MS protocols of this study are described in detail in the supplementary material.

RESULTS AND DISCUSSION

MAIMS EVALUATION

To determine which of the stopping rules defined above is most suitable for obtaining the true g0, r0, a0, u0, u1 and u2 contributions in a reliable manner, yet without excessive computational effort, we compared their behavior on the evaluation datasets (see method section). The results of this comparison can be found in supplementary tables 2, 4 and 6. All runtimes reported hereafter were obtained on an i7-3840QM CPU @ 2.80GHz machine running Ubuntu 16.04.1.

Applying the *I/ROA (5000/20)* stopping rule robustly allowed finding the correct results. For the theoretical datasets, the correct g0, r0, a0, u0, u1 and u2 contributions are obtained in all cases. However, the challenge for these datasets is relatively small considering the large regions of attraction of the global minimum: 59.1% ($d1.t$), 99.7% ($d2.t$) and 39.4% ($d3.t$). For the random datasets, we obtained metabolite concentrations for which deviations from the original values increase with increasing importance of randomization, indicating that the global minimum is also likely to found. Moreover, when the same deconvolution is repeated with different random seeds, the final values are identical, which strengthens the presumption of correctness, despite the often much smaller regions of attraction for the randomized datasets, e.g.: 0.02% ($d1.r3$), 1% ($d1.r4$), 0.1% ($d1.r6$), 0.3% ($d2.r8$) and 0.7% ($d3.r5$). However, despite the correctness of the results, even in the case of many small local minima, we observed as a downside that the I/ROA stopping rule is occasionally overly conservative and lead to excessively long runtimes (e.g. $d1.r3$). Also in cases where the global minimum is obvious (e.g. $d1.t$, $d2.t$, $d2.r2$, etc.) too many iterations are clearly performed.

Compared to I/ROA (5000/20), the *Boender3 (10000)* rule allows to find the same correct results with considerably shorter run times. However, in situations of numerous small local minima, the rule shows lack of stability and consistency. Under such circumstances, it is highly likely that from the beginning on, ten new minima are obtained in ten consecutive iterations, resulting in a continuous increase of $E(L_3)$ and thus an immediate halt of the search. This can be observed for datasets $d1.r2$, $d1.r3$, $d1.r5$, $d1.r6$, $d1.r7$, $d2.r3$, $d2.r8$, $d3.r5$, $d3.r6$, $d3.r7$ and $d3.r8$. Even though the resulting error on the output is limited in these examples, such behavior is obviously not desirable.

The most advanced of the three rules, the *HCS (0.4/0.4)* stopping rule, consistently led to very robust results. Moreover, in comparison to the I/ROA (5000/20) rule, it is also fast in straightforward cases with large global minima (e.g. $d1.t$, $d2.t$, $d2.r2$, etc.). However, in case of small global minima, HCS (0.4/0.4) can also be overly conservative, although not necessarily for the same input data for which I/ROA (5000/20) is excessively slow (e.g. $d1.r6$, $d1.r7$,

$d3.r7$ and $d3.r8$). This effect is especially pronounced for dataset $d3.r8$, where almost seven hours of calculation time were required to obtain the same results which I/ROA (5000/20) could obtain in less than one minute.

When comparing the performances of the stopping rules I/ROA (5000/20) and HCS (0.4/0.4), it can be observed that the faster one of the two is always sufficient to obtain the correct end results and that going beyond the smallest suggested number of iterations does not result in more preciseness. We therefore implemented a hybrid I/ROA - HCS stopping rule in the MAIMS deconvolution tool. Whichever rule cues on performing no additional optimization iterations first, makes the procedure halt. Both rules were used with the default values mentioned above for their working parameters.

As for the Multistart algorithm, several observations corroborate the assumption that it is highly suited for solving the (UDP-GlcNAc) isotopologue deconvolution problem. First, there is a perfect match between the proposed moiety enrichment values and the corresponding enrichments obtained with MAIMS from the theoretical isotopologue profiles. Also the enrichment values obtained from the lower randomized datasets (random 1-4), characterized by small standard deviations (0.001 and 0.002), are in excellent agreements with the initial values. This indicates that MAIMS is insensitive to small errors occurring during measurement. Even at a standard deviation of 0.01 (random 5-6), similar incorporation magnitudes are obtained, which still lead to correct biological conclusions. Only at the large measuring errors (random 7-8, standard deviation: 0.1), deconvolution results may be obtained which are not in line with the initial values (e.g. $d3.r7$ and $d3.r8$). Furthermore, the observation that repeated MAIMS deconvolutions (with different random seeds) consistently result in identical solutions demonstrates the aptitude of MAIMS for the isotopologue deconvolution task.

A TIMES SERIES EXPERIMENT IN ENDOTHELIAL CELLS

We applied MAIMS to UDP-GlcNAc isotopologues from proliferating endothelial cells (ECs) measured at different time points after U-^{13}C-glucose administration (Fig. 2 and supplementary material). Interestingly, the incorporation of U-^{13}C-ribose takes place concurrently with the U-^{13}C-glucose incorporation, reflecting high PPP activity. Furthermore, the [13]C$_2$-uracil incorporation is superior to the incorporation of [13]C$_2$-acetyl, even though UTP is further downstream from glucose than acetyl-CoA and despite ECs being highly glycolytic (De Bock et al. 2013). This can be explained by (a) the conversion of a considerable fraction of glycolytically generated pyruvate to oxaloacetate (using pyruvate carboxylase), which via aspartate results in [13]C$_2$-uracil, while (b) generating acetyl-CoA predominantly through the

degradation of fatty acids (Schoors et al. 2015). Finally, proliferating ECs are known to have low TCA cycle activity (De Bock et al. 2013), which is again reflected here in the slower incorporation of $^{13}C_1$-(1 TCA cycle)- and $^{13}C_3$-(2 TCA cycles)-uracil moieties.

CONCLUDING REMARKS

Stable isotope resolved metabolomics has become a key tool for pathway and flux analysis in cells and multicellular organisms. It has lead to the discovery of numerous metabolites, pathways and regulatory mechanisms in a multitude of biological systems. A further advancement of this field is tightly linked to progress in development of dedicated software tools. With the development of MAIMS, we have made the powerful SIRM analysis concept of isotopologue deconvolution available to a large audience. MAIMS is robust and easily operated and because of the central nutrient sensing role of UDP-GlcNAc, allowed to make several interesting findings in the case study of endothelial cell metabolism. Because a deconvolution model is defined in a separate XML file, MAIMS is also easily extendible. The tool can be obtained from: http://github.com/savantas/MAIMS

ACKNOWLEDGEMENTS

COMPLIANCE WITH ETHICAL STANDARDS

FUNDING

CONFLICT OF INTEREST

The authors declare that they have no conflict of interest.

ETHICAL APPROVAL

All procedures performed in this study involving human participants were in accordance with the ethical standards of the institutional and/or national research committee and with the 1964 Helsinki declaration and its later amendments or comparable ethical standards.

REFERENCES

Banerjee, P. S., Lagerlof, O., & Hart, G. W. (2016). Roles of O-GlcNAc in chronic diseases of aging. *Mol Aspects Med, 51*, 1-15, doi:10.1016/j.mam.2016.05.005.

Boender, C. G. E., & Kan, A. H. G. R. (1987). Bayesian Stopping Rules for Multistart Global Optimization Methods. *Mathematical Programming, 37*(1), 59-80, doi:Doi 10.1007/Bf02591684.

Bond, M. R., & Hanover, J. A. (2015). A little sugar goes a long way: the cell biology of O-GlcNAc. *J Cell Biol, 208*(7), 869-880, doi:10.1083/jcb.201501101.

Buescher, J. M., Antoniewicz, M. R., Boros, L. G., Burgess, S. C., Brunengraber, H., Clish, C. B., et al. (2015). A roadmap for interpreting (13)C metabolite labeling patterns from cells. *Curr Opin Biotechnol, 34*, 189-201, doi:10.1016/j.copbio.2015.02.003.

Dassanayaka, S., & Jones, S. P. (2014). O-GlcNAc and the cardiovascular system. *Pharmacol Ther, 142*(1), 62-71, doi:10.1016/j.pharmthera.2013.11.005.

De Bock, K., Georgiadou, M., Schoors, S., Kuchnio, A., Wong, B. W., Cantelmo, A. R., et al. (2013). Role of PFKFB3-driven glycolysis in vessel sprouting. *Cell, 154*(3), 651-663, doi:10.1016/j.cell.2013.06.037.

Dick, T. W., Eric; Dann, Christoph (2014). How many random restarts are enough?

Hardiville, S., & Hart, G. W. (2014). Nutrient regulation of signaling, transcription, and cell physiology by O-GlcNAcylation. *Cell Metab, 20*(2), 208-213, doi:10.1016/j.cmet.2014.07.014.

Jones, E. O., Travis; Peterson, Pearu (2001 -). Scipy: Open source scientific tools for Python.

Joyner, D., Certik, O., Meurer, A., & Granger, B. E. (2012). Open source computer algebra systems: SymPy. *ACM Commun. Comput. Algebra, 45*(3/4), 225-234, doi:10.1145/2110170.2110185.

Ma, J., & Hart, G. W. (2013). Protein O-GlcNAcylation in diabetes and diabetic complications. *Expert Rev Proteomics, 10*(4), 365-380, doi:10.1586/14789450.2013.820536.

Marti, R., Resende, M. G. C., & Ribeiro, C. C. (2013). Multi-start methods for combinatorial optimization. *European Journal of Operational Research, 226*(1), 1-8, doi:10.1016/j.ejor.2012.10.012.

Moseley, H. N., Lane, A. N., Belshoff, A. C., Higashi, R. M., & Fan, T. W. (2011). A novel deconvolution method for modeling UDP-N-acetyl-D-glucosamine biosynthetic pathways based on (13)C mass isotopologue profiles under non-steady-state conditions. *BMC Biol, 9*, 37, doi:10.1186/1741-7007-9-37.

Ruan, H. B., Singh, J. P., Li, M. D., Wu, J., & Yang, X. (2013). Cracking the O-GlcNAc code in metabolism. *Trends Endocrinol Metab, 24*(6), 301-309, doi:10.1016/j.tem.2013.02.002.

Schoors, S., Bruning, U., Missiaen, R., Queiroz, K. C. S., Borgers, G., Elia, I., et al. (2015). Fatty acid carbon is essential for dNTP synthesis in endothelial cells. *Nature, 520*(7546), 192-U113, doi:10.1038/nature14362.

Singh, J. P., Zhang, K. S., Wu, J., & Yang, X. Y. (2015). O-GlcNAc signaling in cancer metabolism and epigenetics. *Cancer Letters, 356*(2), 244-250, doi:10.1016/j.canlet.2014.04.014.

Wani, W. Y., Chatham, J. C., Darley-Usmar, V., McMahon, L. L., & Zhang, J. (2016). O-
GlcNAcylation and neurodegeneration. *Brain Res Bull*,
doi:10.1016/j.brainresbull.2016.08.002.

1
2
3
4
5
6
7
8
9
10
11
12
13
14
15
16
17
18
19
20
21
22
23
24
25
26
27
28
29
30
31
32
33
34
35
36
37
38
39
40
41
42
43
44
45
46
47
48
49
50
51
52
53
54
55
56
57
58
59
60
61
62
63
64
65

LEGENDS TO THE FIGURES AND TABLES

FIGURE 1: THE PATHWAY DEPENDENCY OF THE INCORPORATION OF GLUCOSE CARBONS IN UDP-GLCNAC.

UDP-GlcNAc consists of four connected carbon-bearing components (glucose (**G**), ribose (**R**), acetyl (**A**) and uracil (**U**)), which may all derive from glucose. The glucose moiety is incorporated via fructose 6-phosphate (F6P), obtained after two glycolysis steps, which then runs through the hexosamine biosynthesis pathway (HBP). The ribose incorporation is mainly dependent on pentose phosphate pathway (PPP) activity in which the necessary ribose 5-phosphate (R5P) is generated. Acetyl is added to UDP-GlcNAc via Acetyl-CoA, which is formed from pyruvate, an end product of glycolysis. The synthesis of uracil relies on pyrimidine biosynthesis pathway activity and its influx of oxaloacetate (OAA). OAA can be generated from pyruvate either directly through pyruvate carboxylase (PC) activity or via TCA cycle intermediates.
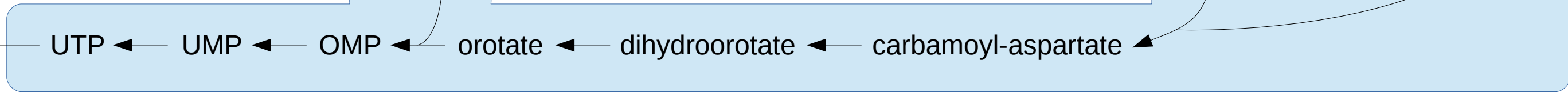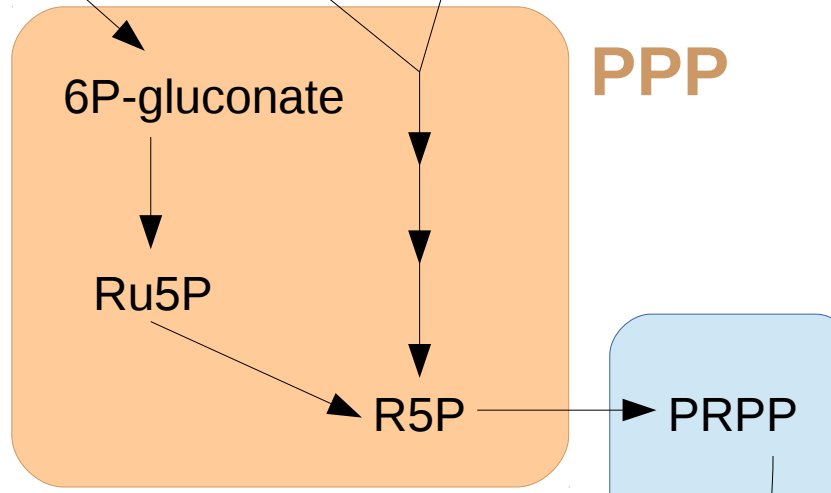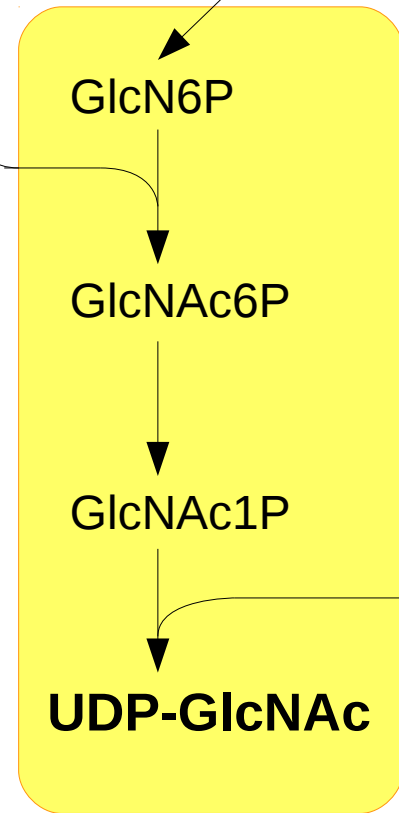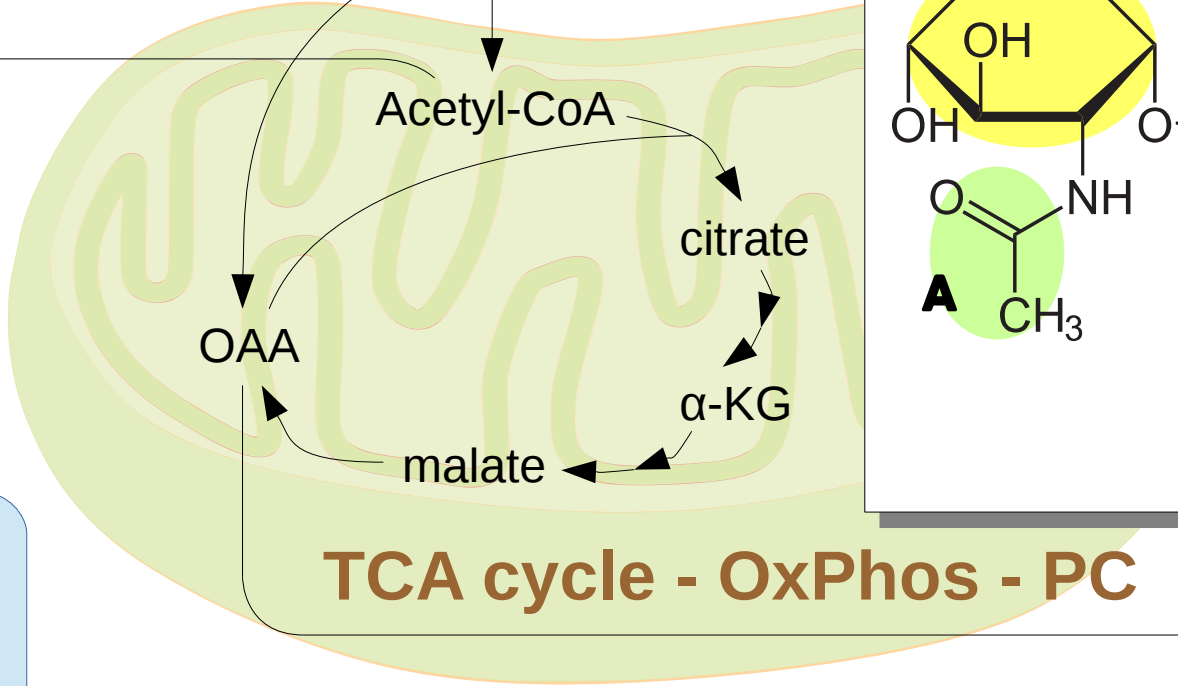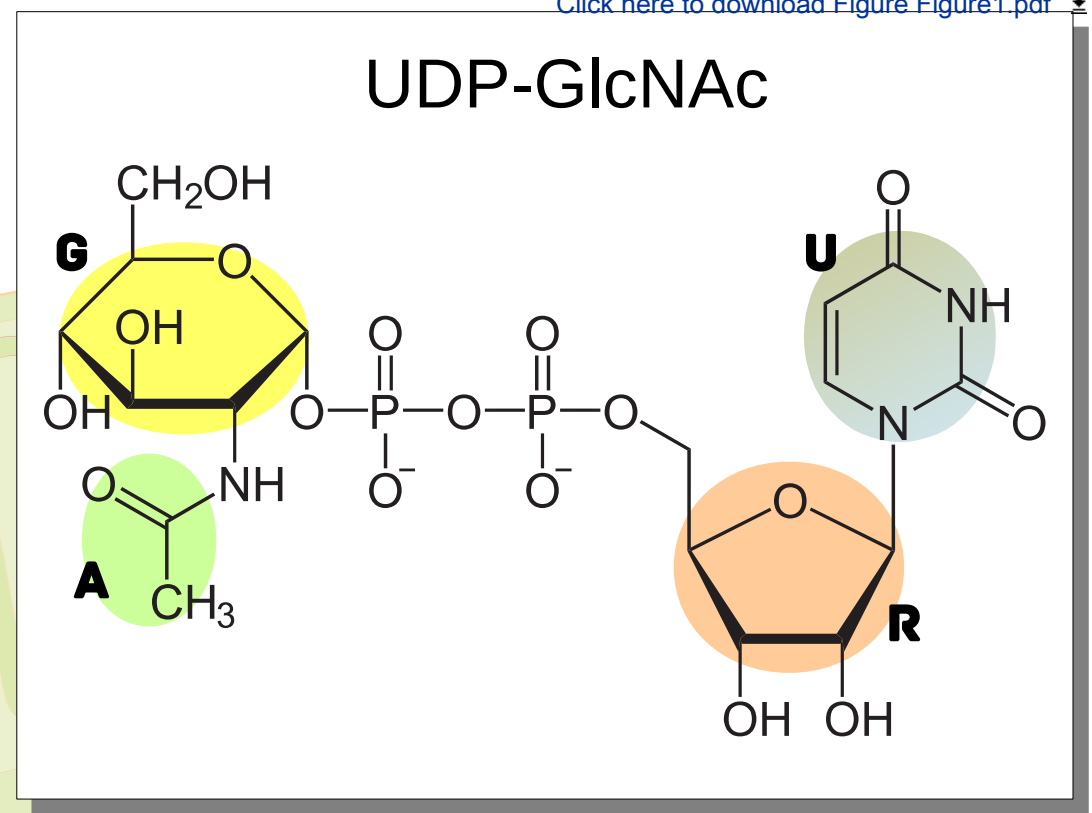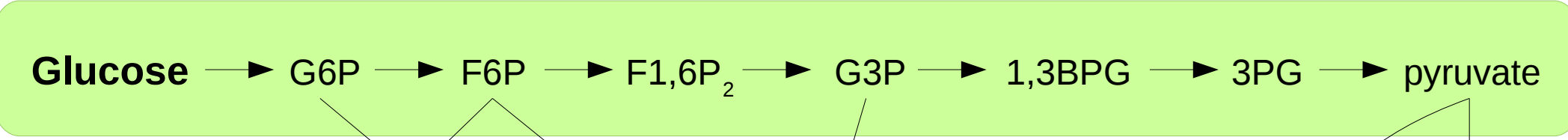
FIGURE 2: TIME-RESOLVED UDP-GLCNAC ISOTOPOLOGUE DECONVOLUTION IN ENDOTHELIAL CELLS.

The temporal incorporation in UDP-GlcNAc of $^{13}C_6$-glucose, $^{13}C_5$-ribose, $^{13}C_2$-acetyl and $^{13}C_1$-, $^{13}C_2$- and $^{13}C_3$-uracil in proliferating ECs upon $^{13}C_6$-glucose administration as calculated from isotopologue profiles using MAIMS. The time points connected by full lines correspond to the mean of two technical repeats, while the error (standard deviation) is represented by the semi-transparent areas. $^{13}C_6$-glucose, directly administered to the cells, is quickly incorporated. The incorporation of most other moieties is slower since their availability depends on the activity of a range of biochemical pathways.

Figure1

Glycolysis

Glucose → G6P → F6P → F1,6P$_2$ → G3P → 1,3BPG → 3PG → pyruvate

PPP

GlcN6P

6P-gluconate

GlcNAc6P

Ru5P

GlcNAc1P

R5P → PRPP

UDP-GlcNAc

TCA cycle - OxPhos - PC

Acetyl-CoA

citrate

OAA

α-KG

malate

Asp

Carbamoyl-P

UTP ← UMP ← OMP ← orotate ← dihydroorotate ← carbamoyl-aspartate

Hexosamine Biosynthesis Pathway

Pyrimidine Biosynthesis

UDP-GlcNAc

CH$_2$OH

G OH

OH OH

A CH$_3$
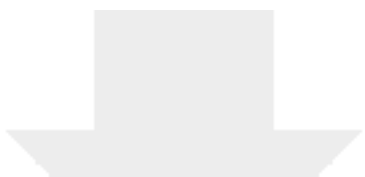
NH

U NH

R OH OH

Figure2
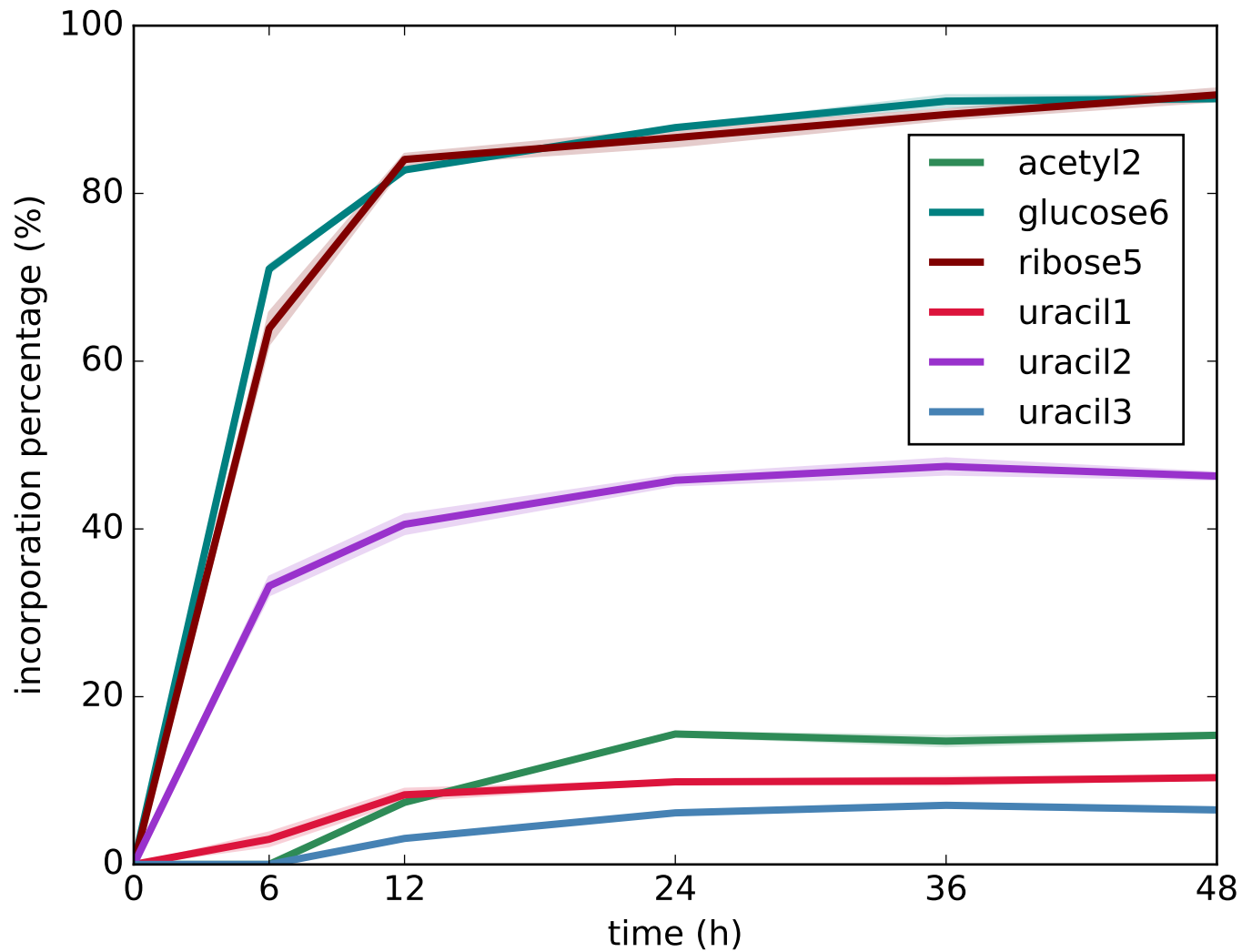
Click here to access/download
Supplementary Material
supplement.pdf

MAIMS code

Click here to access/download
Supplementary Material
MAIMS.zip